Oct 15th, 12:00 AM

Shift of the Effective Centroid of Channel Columns

Ben Young

Kim J. R. Rasmussen

Fourteenth International Specialty Conference on Cold-Formed Steel Structures
St. Louis, Missouri U.S.A., October 15-16, 1998

SHIFT OF THE EFFECTIVE CENTROID OF CHANNEL COLUMNS

Ben Young[†] & Kim J. R. Rasmussen*

ABSTRACT

In the design of pin-ended channel columns, it is necessary to account for the shift of the effective centroid caused by local buckling. The current American Iron and Steel Institute (AISI 1996) Specification and the Australian/New Zealand Standard (AS/NZS 4600-1996) for cold-formed steel structures calculate the shift by use of effective widths. However, the ability of the effective width rules to accurately predict this shift has not been experimentally assessed. In this paper, recent tests on fixed-ended channel columns are used to obtain values of the shift of the effective centroid, including its variation with the applied load. In the tests, the minor axis bending moment was measured at each end, allowing the shift of the effective centroid to be calculated as the ratio of the end moment to the applied force. The shift of the effective centroid, as predicted by the AISI Specification and the AS/NZS 4600 Standard, was shown to be inaccurate compared to the tests on lipped channels with slender flanges. This led to the abnormal result of an *increase* in column strength with *increasing* length in the design of pin-ended columns.

The purpose of this paper is to use test results for plain and lipped channels to assess the ability of the effective width rules of the current AISI Specification and the AS/NZS 4600 Standard for cold-formed steel structures to predict the direction and magnitude of the shift of the effective centroid. When channel columns are loaded eccentrically from the effective centroid, the AISI Specification requires that the member be designed as a beam-column. In this case, the moment capacity calculation depends on the direction of the shift of the effective centroid and so it becomes important to predict the shift accurately both in terms of magnitude and direction. The paper proposes simple modifications to the current effective width rules that provide agreement between the measured and predicted shifts of the effective centroid.

1 INTRODUCTION

Local buckling is a major consideration in the design of thin-walled structures, notably cold-formed structures. The main effect of local buckling is to cause a redistribution of the longitudinal stress in which the greatest portion of the load is carried near the plate junctions, as shown for a plain channel section in Figs 1a and 1b. The redistribution produces increased stresses near the plate junctions and high bending stresses as a result of plate flexure, leading to ultimate loads below the squash load of the section. However, in singly symmetric cross-sections, the redistribution of longitudinal stress caused by local buckling also produces a shift

[†] Senior Researcher, Department of Civil Engineering, University of Sydney, N.S.W. 2006, Australia.
* Senior Lecturer, Department of Civil Engineering, University of Sydney, N.S.W. 2006, Australia.

of the line of action of the internal force, as shown in Figs 1a and 1b. When the section is compressed between pinned ends, this shift, also referred to as the "shift of the effective centroid", introduces an eccentricity and hence overall bending.

Overall bending induced by local buckling can significantly reduce the column strength and needs to be considered in design. This leads to a beam-column design approach, in which the applied moment is calculated as a product of the axial force and its eccentricity. The design eccentricity is found by determining the effective widths of each component plate and thus an effective cross-section with distinct centroid, referred to as the "effective centroid", as shown in Fig. 1c. The design eccentricity is determined as the distance from the effective centroid to the applied force.

In the case of lipped channels, the section may also buckle in a distortional mode that involves in-plane buckling of the lips (or edge stiffeners). The effective width rules of the American Iron and Steel Institute (AISI 1996) Specification for flange elements with edge stiffeners were principally derived to produce accurate section strength predictions. This could be achieved with little regard to the actual location of the effective parts of the cross-section, which determine the position of the effective centroid and hence its shift as shown in Fig. 1. The ability of the effective width rules to accurately predict this shift has not been experimentally assessed. In order to measure the shift experimentally as part of recent tests on plain and lipped channel columns (Young and Rasmussen 1998a, 1998b), a set of fixed-ended bearings were devised that allowed the restraining end moments to be measured. By measuring the minor and major axis end moments, as well as the applied load, the shift of the line of action of the applied force could be calculated. This shift corresponded to the shift of the effective centroid.

Using test results for pin-ended lipped channel columns (Young and Rasmussen 1998b), it was shown that the current design rules lead to conservative predictions. This was partly because the direction of the shift of the effective centroid, as predicted by the AISI Specification and the AS/NZS 4600 Standard, was shown to be inaccurate. According to the AISI predictions, the direction of the shift changed with increasing column length, and this led to the abnormal result of an *increase* in column strength with *increasing* length.

Simple modifications to the current design rules for determining the effective widths of uniformly compressed elements with an edge stiffener are proposed in this paper. These modifications do not change the total effective area and hence not the design section strength. However, the proposed modifications lead to accurate predictions of the magnitude and direction of the shift of the effective centroid of lipped channel sections. By using the modified design rules, the predicted pin-ended design strength for lipped channels with slender flanges have been improved and the abnormal results of an increase in column strength with increasing length no longer occurs.

2 SUMMARY OF TEST PROGRAM

The test program described in Young and Rasmussen (1998a, 1998b and 1998d) provided experimental ultimate loads for cold-formed plain and lipped channel columns compressed between fixed ends and pinned ends. All test specimens were brake-pressed from high strength zinc-coated Grade G450 steel sheets with nominal yield stress of 450MPa. The test program comprised four different cross-section geometries, two series of plain channels and two series

of lipped channels. All four cross-sections had a nominal thickness of 1.5mm and a nominal width of the web of 96mm. The nominal width of the lip of both lipped channels was 12mm. The nominal flange width was either 36mm or 48mm and was the only variable in the cross-section geometry. Accordingly, the four test series were labelled P36, P48, L36 and L48 where "P" and "L" refer to "plain" and "lipped" channel respectively. The specimens were tested between fixed ends and pinned ends at various column lengths. The pin-ended specimens were tested using the same effective lengths as those for the fixed-ended specimens.

The average values of measured cross-section dimensions of the fixed-ended and pin-ended test specimens are shown in Table 1 using the nomenclature defined in Fig. 2. The shortest column lengths complied with the guidelines (Galambos, 1988) of the Structural Stability Research Council (SSRC) for stub column lengths, while the longest lengths produced l_{ey}/r_y -ratios of approximately 130, 110, 110 and 100 for Series P36, P48, L36 and L48 respectively, where l_{ey} is the *effective* length for buckling about the minor y-axis and r_y is the radius of gyration about the y-axis. The measured cross-section dimensions of each specimen are detailed in Young and Rasmussen (1998a, 1998b and 1998d).

The material properties determined from coupon tests are summarised in Table 2. The table contains the nominal 0.2% tensile proof stress ($\sigma_{0.2}$), the measured static 0.2% ($\sigma_{0.2}$) and 0.5% ($\sigma_{0.5}$) tensile proof stresses, the tensile strength (σ_u) as well as the Young's modulus (E) and the elongation after fracture (ε_u) based on a gauge length of 50mm. The stress-strain curves obtained from the coupon tests are detailed in Young and Rasmussen (1998a and 1998b). Two separate specimens from Series L48 were prepared for residual strain measurement by attaching strain gauges around half of the cross-section on the outer and inner surfaces. The *membrane* and the *flexural* residual stresses were calculated as the average and the difference in residual stress measurements at the two surfaces respectively, and were found to be less than 3% and 7% of the measured 0.2% tensile proof stress ($\sigma_{0.2}$) respectively. Hence, the residual stresses were deemed negligible compared with $\sigma_{0.2}$. Full details of the residual stress measurements are given in Young and Rasmussen (1995b).

Local and overall geometric imperfections were measured for both the fixed-ended and pin-ended columns. The measured maximum local imperfections were found to be of the order of the plate thickness at the tip of the flanges for all test series. For the fixed-ended specimens, the maximum overall minor axis flexural imperfections at mid-length were 1/1400, 1/2500, 1/1100 and 1/1300 of the specimen length for Series P36, P48, L36 and L48 respectively. For the pin-ended specimens, the maximum minor axis flexural imperfections at mid-length were 1/2200, 1/5000, 1/1800 and 1/2800 of the specimen length for Series P36, P48, L36 and L48 respectively. The recording procedure and reduction of the imperfection measurement as well as the measured local and overall geometric imperfection profiles are detailed in Young and Rasmussen (1995a and 1995b).

A 250kN servo-controlled hydraulic actuator was used to apply compressive axial force to the specimen. The pin-ended bearings were designed to allow rotations about the minor axis while restraining major axis rotations as well as twist rotations and warping. The fixed-ended bearings were designed to restrain both minor and major axis rotations as well as twist rotations and warping. Details of the test rig are given in Young and Rasmussen (1995a and 1998c).

3 MEASUREMENT OF THE SHIFT OF THE EFFECTIVE CENTROID

A set of fixed-ended bearings were devised that allowed the restraining end moments to be measured (Young and Rasmussen 1995b). By measuring the external minor and major axis bending moments at the ends, as well as the applied load, the internal bending moments in the specimen could be determined statically. The shift in the line of action of the internal force resulting from local buckling could then be determined as the ratio of the end moment to the applied force.

Figure 3 shows a schematic view of the fixed-ended bearings. A photograph of the fixed-ended bearings is shown in Fig. 4. A series of compression springs round the circumference allowed the "top plate" of each bearing to slide in the direction of loading during setup to provide full contact with the specimen, as shown in Figs 3a and 3b. Eight high strength bolts were tightened evenly to lock the top plate in position after full contact was achieved, thus ensuring a fully fixed support. The "side plates" were used to restrain twist rotations of the top plate. Four strain gauges were attached to each of the four steel rods of each bearing and connected in series to eliminate bending effects within each rod. The steel rods were calibrated prior to testing to allow the load in each rod, and hence the applied axial force and the restraining end moments, to be measured during the tests.

4 CURRENT EFFECTIVE WIDTH DESIGN RULES

The AISI design rules for determining the effective width of a uniformly compressed element with an edge stiffener are summarised in this section. The AS/NZS 4600 Standard has adopted its effective width design rules from the AISI Specification, and so the following summary also applies to the AS/NZS 4600 Standard.

Three cases are used for determining the effective widths ($C_1b/2$, $C_2b/2$) of a uniformly compressed element with an edge stiffener. The factors C_1 and C_2 determine the portions of the effective width (b) located at the supported and lip-stiffened edges respectively, as shown in Fig. 5a. According to Section B2.1 of the AISI Specification, the total effective width is given by the Winter equation (1968),

$$\frac{b}{w}=\begin{cases} 1 & \text{when} \quad \lambda \le 0.673 \\ \dfrac{\left(1-\dfrac{0.22}{\lambda}\right)}{\lambda} & \text{when} \quad \lambda > 0.673 \end{cases} \qquad (1)$$

where w is the flat width of element excluding the corner radii, as shown in Fig. 5b. The slenderness factor (λ) is given by,

$$\lambda=\frac{1.052}{\sqrt{k}}\left(\frac{w}{t}\right)\sqrt{\frac{f}{E}} \qquad \text{[AISI Eq. B2.1-4]} \quad (2)$$

where k is the plate buckling coefficient as determined in equation (11), t is the plate thickness, f is the design stress in the compression element calculated on the basis of the effective width, and E is the Young's modulus of elasticity.

The design rules for strength calculations of the factors (C_1, C_2) and the effective width (d_s) of a simple lip stiffener according to Section B4.2 of the AISI Specification are as follows,

Case I: $\frac{w}{t} \le \frac{S}{3}$

$$I_a = 0 \text{ (no edge stiffener is required)} \tag{3}$$

$$b = w \qquad \text{[AISI Eq. B4.2-1]} \tag{4}$$

$$d_s = d_s' \qquad \text{[AISI Eq. B4.2-2]} \tag{5}$$

Case II: $\frac{S}{3} < \frac{w}{t} < S$

$$\frac{I_a}{t^4} = 399\left[\frac{\left(\frac{w}{t}\right)}{S} - \sqrt{\frac{k_u}{4}}\right]^3 \qquad \text{[AISI Eq. B4.2-4]} \tag{6}$$

$$I_s = \frac{d^3 t \sin^2 \theta}{12} \quad \text{(for stiffener shown in Fig. 5b)} \qquad \text{[AISI Eq. B4-2]} \tag{7}$$

$$C_2 = \frac{I_s}{I_a} \le 1 \qquad \text{[AISI Eq. B4.2-5]} \tag{8}$$

$$C_1 = 2 - C_2 \qquad \text{[AISI Eq. B4.2-6]} \tag{9}$$

where

$$k_u = 0.43 \tag{10}$$

The buckling coefficient (k) and the effective width of the lip (d_s) are determined using,

$$k = C_2^n (k_a - k_u) + k_u \qquad \text{[AISI Eq. B4.2-7]} \tag{11}$$

$$d_s = C_2 d_s' \qquad \text{[AISI Eq. B4.2-9]} \tag{12}$$

where

$$n = \frac{1}{2} \tag{13}$$

$$k_a = 5.25 - 5\left(\frac{D}{w}\right) \le 4.0 \qquad \text{[AISI Eq. B4.2-8]} \quad (14)$$

Equations (12) and (14) apply in the ranges $D/w \le 0.8$ and $40° \le \theta \le 140°$.

Case III: $\frac{w}{t} \ge S$

$$\frac{I_a}{t^4} = \left[\frac{115\left(\frac{w}{t}\right)}{S}\right] + 5 \qquad \text{[AISI Eq. B4.2-11]} (15)$$

The quantities C_1, C_2, b, k and d_s shall be calculated according to Case II with n = 1/3 in equation (11) [AISI Eq. B4.2-7].

In Cases I, II and III,

$$S = 1.28\sqrt{\frac{E}{f}} \qquad \text{[AISI Eq. B4-1]} \quad (16)$$

In the equations above, d_s and d_s' are the reduced (final) and actual effective width of stiffener respectively, as shown in Fig. 5b, D and d are the overall and flat width of lip respectively, θ is the angel between the element and its edge stiffener, I_a is the "adequate" second moment of area of the stiffener so that each component element behaves as a stiffened element, and I_s is the second moment of area of the full stiffener about its own centroidal axis parallel to the element that it stiffened.

5 COMPARISON OF MEASURED AND PREDICTED SHIFTS OF THE EFFECTIVE CENTROID

The shift of the effective centroid (e_s) predicted by the AISI Specification and the AS/NZS 4600 Standard is plotted against the minor axis effective length for plain and lipped channels in Figs 6a and 6b respectively (Young and Rasmussen 1998a and 1998b). The shift was calculated as the distance between the geometric centroid and the centroid of the effective cross-section determined at the *ultimate* design load. The design predictions are compared with the measured values of e_s, determined as the average of the ratios of measured minor axis end moments to axial load at ultimate for the fixed-ended columns. The end moments at ultimate of each specimen are detailed in Young and Rasmussen (1995a and 1995b). The measured shifts are plotted using open and closed markers, where the open markers are used when the end moments differed by more than 15%. The shifts shown with open markers are considered less reliable than those shown with solid markers because of the difficulty of defining a load eccentricity in the presence of a moment gradient.

For plain channel sections, the predicted effective centroid shifts toward the web (negative values of e_s) at all effective lengths for the Series P36 and Series P48 sections, as shown in Fig.

6a. The shift of the effective centroid increases as the effective length decreases leading to higher design stresses, and this was generally supported by the tests. The comparison shown in Fig. 6a demonstrates that the shifts obtained using the current effective width rules are over-estimated. This leads to conservative design strengths for the pin-ended columns (Young and Rasmussen 1998a and 1998d).

For the lipped channel Series L36 section, the predicted effective centroid shifts toward the lips (positive values of e_s) at all effective lengths, as shown with a thick solid line in Fig. 6b. At long lengths, the shift occurs as a result of local buckling of the web only. The magnitude of the shift increases as the effective length decreases (because the ultimate load increases and so reduces the effective area of the web), until an effective length of approximately 750mm where the flange and lip become unstable causing the effective centroid to shift back towards its initial position. The variation at short lengths was supported by the tests. However, the tests indicated a small shift toward the web at intermediate lengths (negative values of e_s) rather than toward the lip as predicted by the design specifications.

For the Series L48 section, the predicted effective centroid shifts toward the lips at long lengths until the flange and lips become unstable at an effective length of approximately 1750mm. As a result of flange and lip buckling, the effective centroid starts shifting toward the web, as shown in Fig. 6b. This variation was not supported by the tests which showed that the centroid shifted toward the lips at all effective lengths. It should be noted that a discontinuity was found in the shift of the effective centroid curve as predicted by the AISI Specification and the AS/NZS 4600 Standard for the Series L48, as shown in Fig. 6b. The discontinuity occurs in changing from Case II (n = 1/2) to Case III (n = 1/3), as discussed by Dinovitzer et al. (1992). Hence, a linear transition for the parameter (n) from 1/2 to 1/3 was used in calculating the effective width of an edge-stiffened flange element, as proposed by Dinovitzer et al. (1992) and applied in Young and Rasmussen (1998b and 1998d). The shift of the effective centroid calculated using the linear transition is plotted in Fig. 6b. The method provided a smooth curve in changing from Case II to Case III.

The measured shift of the effective centroid of the four fixed-ended channel sections at an effective length of 500mm is also presented. The experimentally measured shifts (e_s) of the Series P36, P48, L36 and L48 sections are plotted against the applied load (N) in Figs 7a, 7b, 7c and 7d respectively. The measured values of e_s are calculated as the ratio of the average measured minor axis end moments divided by the measured applied load. The shifts are compared with the shifts predicted using the AISI Specification and the AS/NZS 4600 Standard for channel sections at an effective length of 500mm.

For the plain channel Series P36 and P48 sections, the predicted effective centroid shifts toward the web at any level of loading, as shown in Figs 7a and 7b respectively. The direction of the predicted shift was in agreement with the measured values. At the ultimate load, the measured shifts were 3.2mm and 7.2mm toward the web and the predicted shifts were 3.8mm and 8.3mm toward the web for Series P36 and P48 respectively, indicating good correlation. For the lipped channel Series L36 and L48 sections, the measured effective centroid shifts toward the lips at any level of loading which was the opposite direction to that of the plain channel sections. For the Series L36 section, the direction of the predicted shift was in agreement with the measured values. The measured and the predicted shifts were 3.3mm and 2.2mm toward the lips at the ultimate load respectively. For the Series L48 section, the predicted shift was initially toward the lip but changed at a load of approximately 52kN to shift

toward the web, contrary to the measured shift. At the ultimate load, the measured shift was 2.7mm toward the lips while the predicted shift was 2.0mm toward the web. The inaccuracy of the predicted shift leads to abnormalities in the design strength curves as described in the following section of this paper.

6 DESIGN STRENGTH CURVES

The pin-ended unfactored design strengths predicted using the AISI Specification and the AS/NZS 4600 Standard for cold-formed steel structures are plotted against the effective length for minor axis flexural buckling (l_{ey}) in Fig. 8 for Series L48. The effective length was assumed equal to the column length, which included the dimension of the pin-ended bearings. Two design curves are plotted as dotted lines, one corresponding to loading through the geometric centroid, as was also used in the tests. In this case, the design strengths were calculated using the rules for members in combined bending and compression. This was required because the columns were loaded through the geometric centroid, while the specifications assume concentric loading to be at the centroid of the *effective* cross-section. The end moment was calculated as the product of the axial force and the distance between the geometric and effective centroids. The second design curve (N_c) was plotted corresponding to loading through the effective centroid.

The experimental ultimate loads and the failure modes of each specimen are also plotted in Fig. 8. The failure modes of the tests were those observed at the ultimate load. The Euler buckling loads as well as the experimental local buckling loads are also shown in Fig. 8, as determined in Young and Rasmussen (1995b and 1998d). The design strengths and the theoretical buckling loads were calculated using the average measured cross-section dimensions and the measured material properties detailed in Tables 1 and 2 respectively.

It appears from Fig. 8 that the AISI and AS/NZS 4600 design curves based on a beam-column design procedure predict an *increase* in column strength with increasing length from an effective length of approximately 1100mm to 1350mm. This variation was not supported by the tests, neither does it appear justified from a physical viewpoint. The variation was a result of the shift of the effective centroid which was predicted to decrease rapidly in magnitude between 1100mm and 1350mm, and to be zero at an effective length of about 1350mm, as shown in Fig. 6b. Where the shift was zero, the design strength was that of a column loaded through the effective centroid.

The effective width rules of the AISI Specification for flange elements with edge stiffeners were principally derived to produce accurate section strength predictions, as mentioned in the Introduction. This could be achieved with little regard to the actual location of the effective parts of the cross-section. As shown in Figs 6b and 7d, the rules do not provide accurate predictions of the location of the effective parts of the flanges and lips, since otherwise the predicted shift would have been in agreement with the measured values. As shown in Fig. 8, the inability of the rules to accurately predict the shift of the effective centroid has serious implications for the design strength curves of the AISI Specification and the AS/NZS 4600 Standard.

7 PROPOSED EFFECTIVE WIDTH DESIGN RULES

The shift of the effective centroid predicted by the current design rules was shown to be inaccurate compared to the tests on the lipped channel with slender flanges, as shown in Figs 6b and 7d. The inaccurate prediction can be improved by changing the widths of the effective parts of the flanges $C_1b/2$ and $C_2b/2$, as shown in Fig. 5a. Simple modifications to the current design rules are proposed that change the widths ($C_1b/2$, $C_2b/2$) to produce agreement between the predicted and measured shifts of the effective centroid of the lipped channel section with slender flanges. In the procedure, the total effective area is unchanged so that the design column strength (N_c) remains unchanged. The proposed modifications are summarised as follows:

In equation (8) [AISI Eq. B4.2-5], a positive integer factor i is included to increase the coefficient C_2, and hence the effective flange width near the flange-lip junction.

$$C_2 = i\frac{I_s}{I_a} \le 2 \tag{17}$$

However, the coefficient C_1 is still obtained from Eq. (9) and so the total effective width of the flanges remains equal to b. The expression for C_2 is bounded by the value of 2 rather than 1 as in eqn. (8).

In equations (11) and (12) [AISI Eq. B4.2-7 and B4.2-9], the coefficient C_2 is replaced by the ratio of full to adequate second moment of area of the stiffener (I_s/I_a). As a result, the plate buckling coefficient (k) and the reduced effective width of stiffener (d_s) remain identical to those calculated according to the current design rules. This ensures that the total effective widths of the flange (b) and the lip (d_s) remain unchanged.

$$k = \left(\frac{I_s}{I_a}\right)^n (k_a - k_u) + k_u \tag{18}$$

$$d_s = \left(\frac{I_s}{I_a}\right) d_s' \le d_s' \tag{19}$$

8 COMPARISON OF MEASURED AND PROPOSED SHIFTS OF THE EFFECTIVE CENTROID

Figures 9a and 9b show the shift of the design effective centroid (e_s) for the Series L36 and L48 fixed-ended columns respectively. The shift is based on the modified expressions for the effective widths ($C_1b/2$, $C_2b/2$) and is plotted against the axial load (N). The experimental measured shift (e_s) is also plotted for the fixed-ended columns with effective lengths of 500mm. The experimental local buckling load is included in Fig. 9.

The measured shift is compared with the shift predicted using the proposed design rules with the factor i = 2, 3 and 10 for Series L36 and the factor i = 8, 10 and 12 for Series L48. The Dinovitzer n-parameter together with the factor i = 10 was also used in determining the shift of

the effective centroid for Series L48, as shown in Fig. 9b. The parameter provided a smooth curve in changing from Case II to Case III. The direction of the predicted shift using the proposed design rules was in agreement with the measured values for Series L48 for all three values of i, as shown in Fig. 9b. However, the value $i = 10$ provided overall the best agreement between the predicted and measured shifts. Using $i = 10$ for the Series L48 section at a load level of 100kN, the measured and predicted shifts are 2.5mm and 2.3mm toward the lips respectively, while the predicted shift using the current design rules is 2.5mm toward the web. It is recommended that the Dinovitzer n-parameter together with a factor $i = 10$ be used for calculating the effective width of uniformly compressed elements with an edge stiffener.

To explain the variation of the design shift of the effective centroid, the non-dimensionalised effective widths of each component plate are plotted against the applied axial compressive load in Figs 10a and 10b for Series L36 and L48 respectively. A curve is also shown for the Series L48 section using the Dinovitzer n-parameter to obtain a smooth effective flange width curve. For both sections, the web becomes first unstable, then the lips and finally the flange and lip combined corresponding to distortional buckling. Using the graphs of effective width, the effective cross-sections have been drawn against the applied load in Figs 9a and 9b for Series L36 and L48 respectively.

9 COMPARISON OF TEST STRENGTHS WITH CURRENT AND PROPOSED DESIGN STRENGTHS

In using the design rules for beam-columns to calculate the strength of pin-ended channel columns loaded through the geometric centroid, it is necessary to determine the minor axis bending capacity and the distance between the geometric and effective centroids. The bending capacity depends on whether the web or the lips are in compression and hence on the direction of the shift of the effective centroid (e_s). The difference in bending capacity can be significant for the two directions. For the Series L48 section, the minor axis bending capacities were 763×10^3Nmm and 1601×10^3Nmm when the shift of the effective centroid was toward the web and lips respectively.

According to the current design rules, the effective centroid shifted toward the web at short effective lengths (contrary to the tests), and so the smaller bending capacity was used at short lengths. By using the proposed effective width design rules with a factor $i = 10$, the shift of the effective centroid is always toward the lips and so the larger bending capacity is used at all effective lengths. This leads to an increase in beam-column strength at short lengths, as shown in Fig. 8, and to better agreement between the design strengths and the tests.

The experimental ultimate loads (N_u) obtained for the pin-ended Series L48 columns are compared in Table 3 with the current ($N_{Current}$) and proposed ($N_{Proposed}$) design strength. The current and proposed design strengths were calculated using the average measured cross-section dimensions and the measured material properties detailed in Tables 1 and 2 respectively. The ratios of experimental ultimate load to design strength are closer to unity when using the proposed design rules indicating more accurate design strengths. Using the proposed design rules leads to an increase in design strength of 13.8% at an effective length of 500mm, as shown in Table 3. At long effective lengths, the current and proposed design

strengths are identical, as shown in Fig. 8 and Table 3, because the predicted shifts of the effective centroid calculated using the current and proposed design rules are the same.

10 CONCLUSIONS

The ability of the current design rules to determine accurately the effective width of uniformly compressed elements with an edge stiffener using the American Iron and Steel Institute (AISI) Specification and the Australian/New Zealand Standard (AS/NZS 4600) for cold-formed steel structures has been experimentally assessed. The shift of the effective centroid as predicted by the current design rules was shown to be accurate for plain channels but inaccurate for lipped channel with slender flanges (Series L48 channel). As a result, the current design strength curve for lipped channel with slender flanges *increased* with increasing effective lengths. This abnormality was overcome by using the modifications to the effective width design rules proposed in this paper.

The proposed effective width design rules are simple, and require only small modifications to the current effective width design rules. It is recommended that the Dinovitzer *n*-parameter be used in conjunction with the proposed design rules in calculating the effective width of uniformly compressed elements with an edge stiffener. In using the proposed effective width design rules, the direction of the predicted shift of the effective centroid was in agreement with the measured values. In addition, an increase in the pin-ended column design strength of 13.8% at an effective length of 500mm for Series L48 was obtained by using the proposed effective width design rules.

REFERENCES

American Iron and Steel Institute, (1996). Specification for the Design of Cold-Formed Steel Structural Members. AISI, Washington, DC.

Australian/New Zealand Standard, (1996). Cold-Formed Steel Structures. AS/NZS 4600:1996, Standards Australia, Sydney, Australia.

Dinovitzer, A.S., Sohrabpour, M. and Schuster, R.M., (1992). "Observation and Comments Pertaining to CAN/CSA-S136-M89", Proc. 11th Int. Specialty Conf. on Cold-Formed Steel Struct., St. Louis, Mo, U.S.A., 551-569.

Galambos, T.V., (1988). Ed. *Guide to Stability Design Criteria for Metal Structures.* 4th Edition, Wiley Inc., 708-710.

Winter, G., (1968). "Thin-Walled Structures - Theoretical Solutions and Test Results", Preliminary Publications of the Eighth Congress, Int. Association for Bridge and Structural Engineering (IABSE), 101-112.

Young, B. and Rasmussen, K.J.R., (1995a). Compression Tests of Fixed-ended and Pin-ended Cold-Formed Plain Channels. *Research Report* R714, School of Civil and Mining Engineering, University of Sydney, Australia.

Young, B. and Rasmussen, K.J.R., (1995b). Compression Tests of Fixed-ended and Pin-ended Cold-Formed Lipped Channels. *Research Report* R715, School of Civil and Mining Engineering, University of Sydney, Australia.

Young, B. and Rasmussen, K.J.R., (1998a). "Tests of Fixed-ended Plain Channel Columns", *Journal of Structural Engineering,* ASCE, Vol. 124(2), 131-139.

Young, B. and Rasmussen, K.J.R., (1998b). "Design of Lipped Channel Columns", *Journal of Structural Engineering,* ASCE, Vol. 124(2), 140-148.

Young, B. and Rasmussen, K.J.R., (1998c). "Behaviour of Locally Buckled Singly Symmetric Columns", Proc. 14th Int. Specialty Conf. on Cold-Formed Steel Struct., St. Louis, Mo, USA.

Young, B. and Rasmussen, K.J.R., (1998d). "Tests of Cold-Formed Channel Columns", Proc. 14th Int. Specialty Conf. on Cold-Formed Steel Struct., St. Louis, Mo, USA.

NOTATION

A	Full cross-section area
B_f, B_l, B_w	Overall width of flange, lip and web plate
b	Effective width
C_1, C_2	Coefficients as defined in Fig. 5a
D	Overall width of lip
d	Flat width of lip
d_s	Reduced effective width of stiffener
d_s'	Actual effective width of stiffener
E	Young's modulus of elasticity
e_s	Distance from the point of application of the axial load to the centroid of the effective cross-section (Shift of the effective centroid)
f	Design stress in the compression element calculated on the basis of the effective width
I_a	Adequate second moment of area of the stiffener
I_s	Second moment of area of the full stiffener about its own centroidal axis parallel to the element to be stiffened
i	A positive integer factor used in the proposed design rules
k	Plate buckling coefficient
l_{ey}	Effective length for flexural buckling about the minor axis
N	Applied compressive axial force
N_c	Column design strength (loading through the effective centroid)
$N_{Proposed}$	Proposed design strength pin-ended column (loading through the geometric centroid)
$N_{Current}$	Current design strength for pin-ended column (loading through the geometric centroid)
N_u	Experimental ultimate load
n	Dinovitzer n-parameter
r_i	Inside corner radius of specimen
r_y	Radius of gyration about the minor y-axis

t	Plate thickness
t^*	Base metal plate thickness
w	Flat width of element excluding radii
x	In-plane transverse coordinate
y	Out-of-plane transverse coordinate
ε_u	Elongation (tensile strain) after fracture based on a gauge length of 50mm
λ	Slenderness factor
θ	Angel between an element and its edge stiffener
$\sigma_{0.2}$	Static 0.2% tensile proof stress
$\sigma_{0.5}$	Static 0.5% tensile proof stress
σ_u	Ultimate tensile strength

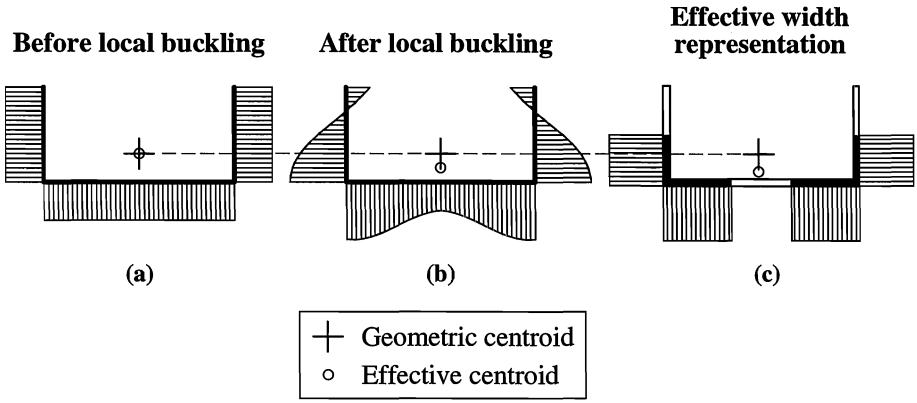

Fig. 1. Stress redistribution of channel section in uniform compression

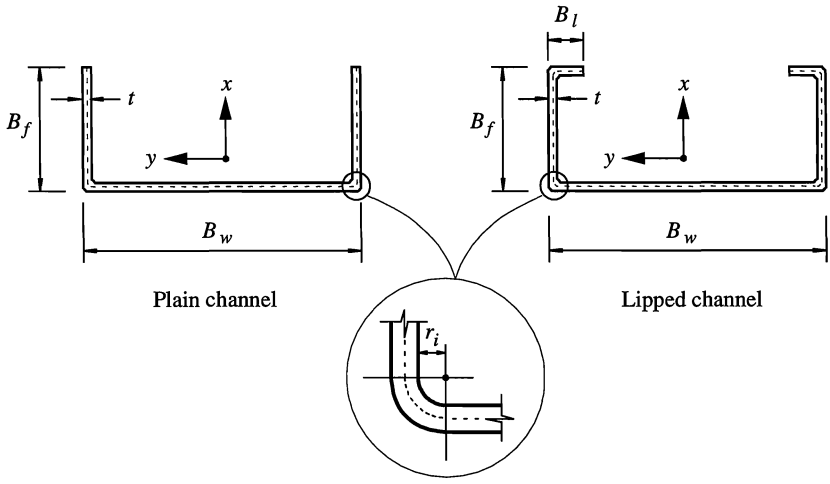

Fig. 2. Definition of symbols

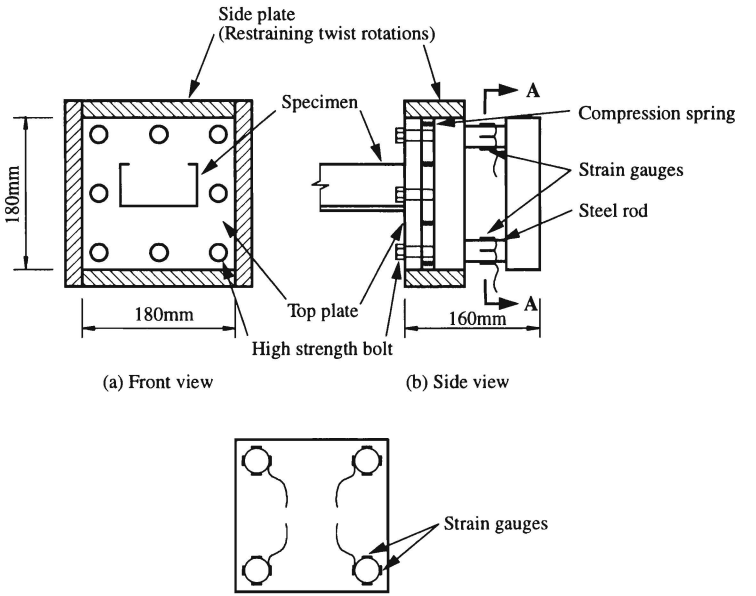

Fig. 3. Details of fixed-ended bearing

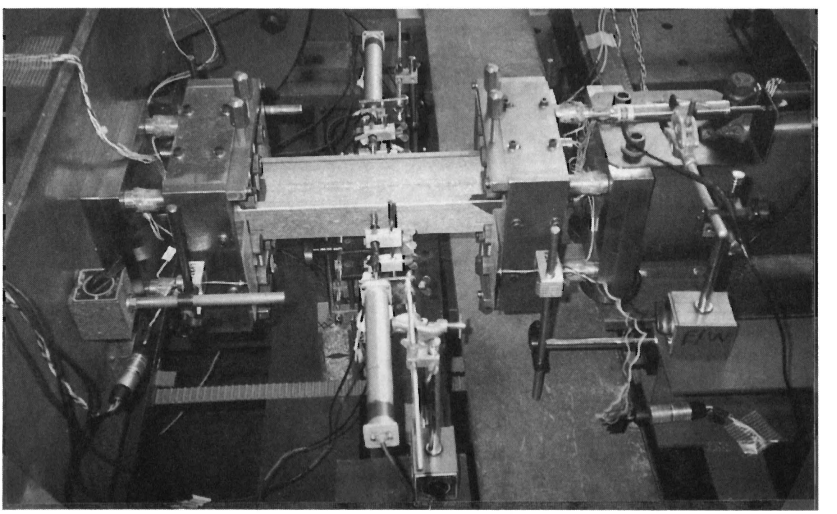

Fig. 4. Test of short specimen and fixed-ended bearing setup

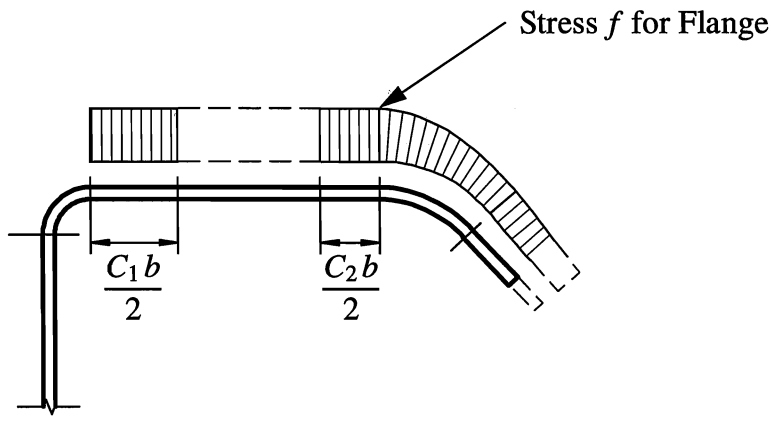

(a) Effective element

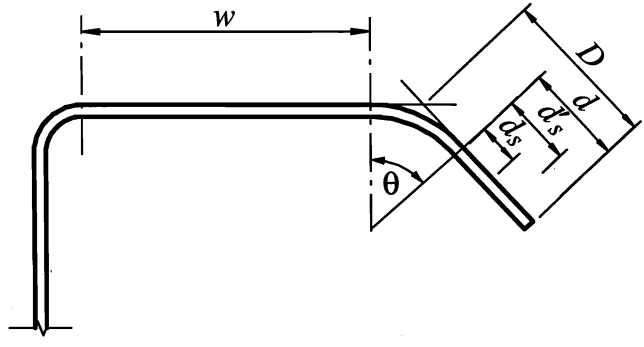

(b) Definition of symbols

Fig. 5. Elements with edge stiffener

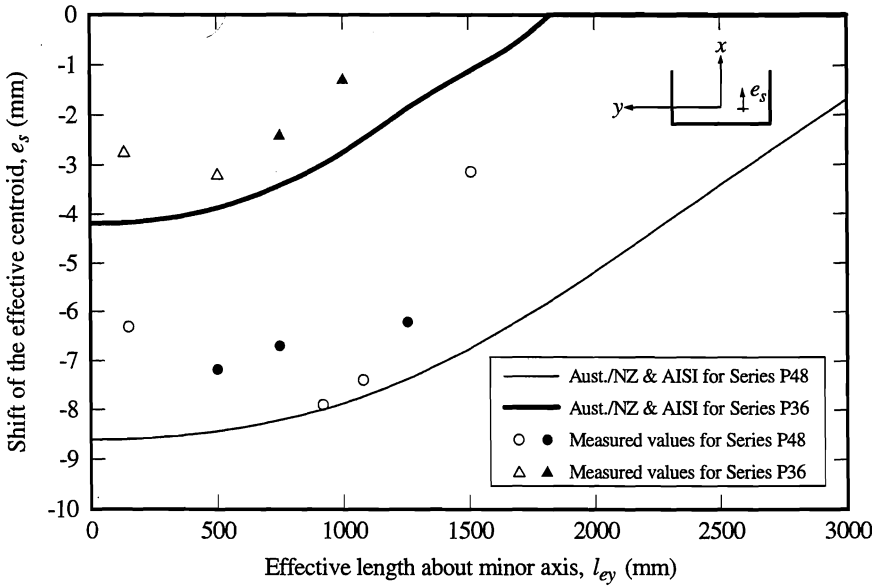

(a) Plain channel

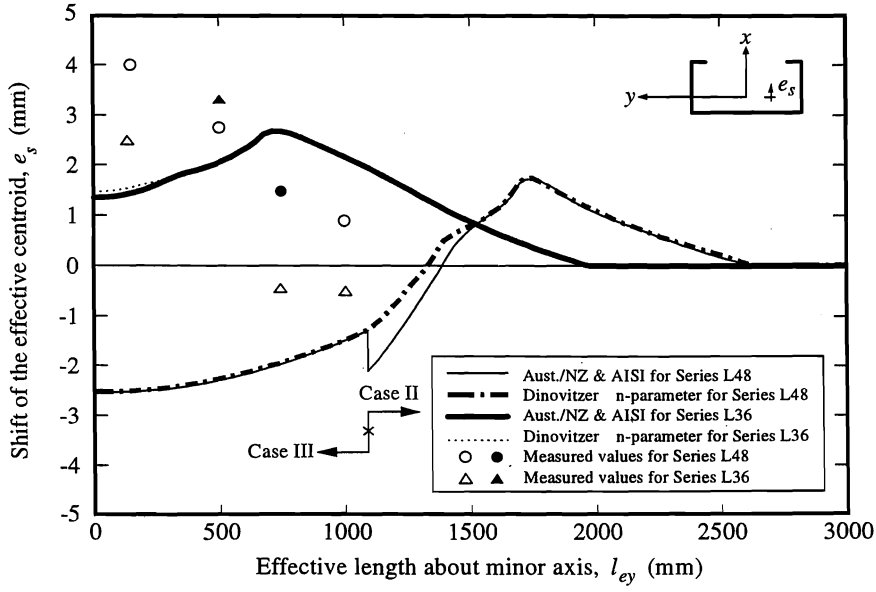

(b) Lipped channel

Fig. 6. Shift of the effective centroid vs effective length

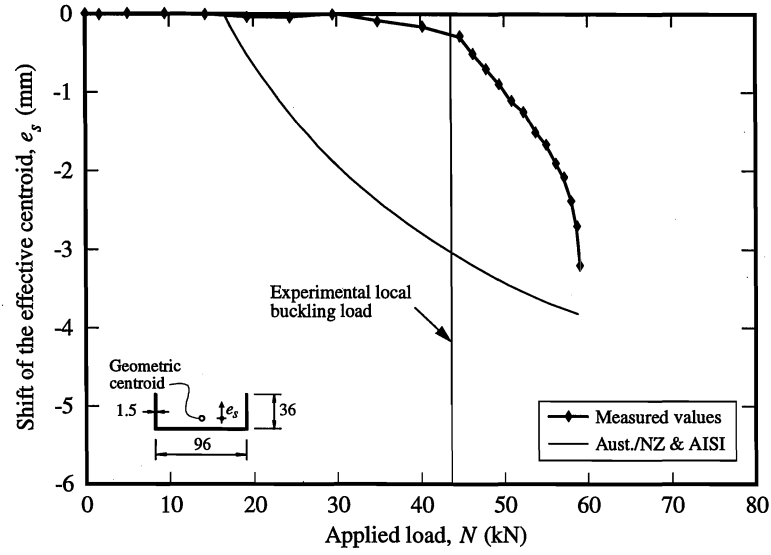

(a) Series P36

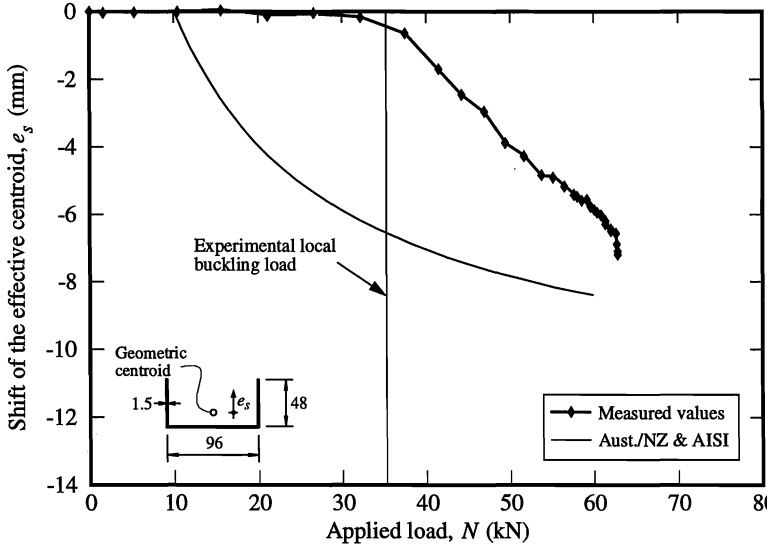

(b) Series P48

Fig. 7. Shift of the effective centroid vs applied load at an effective length of 500mm

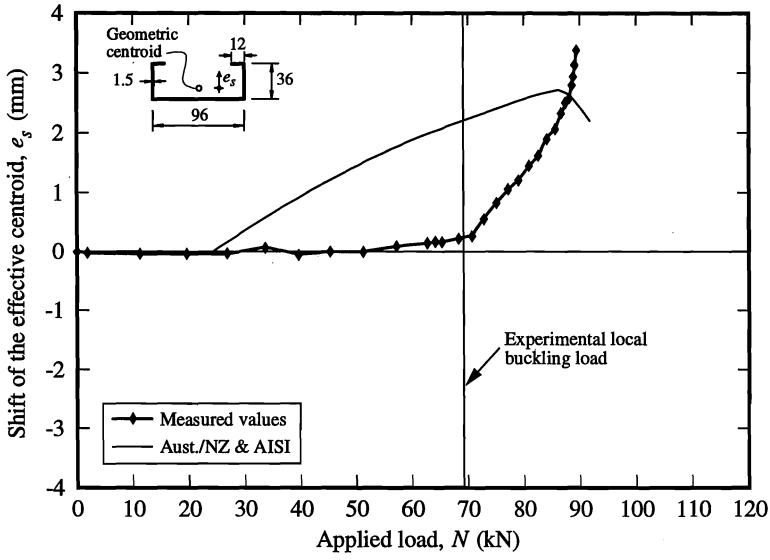

(c) Series L36

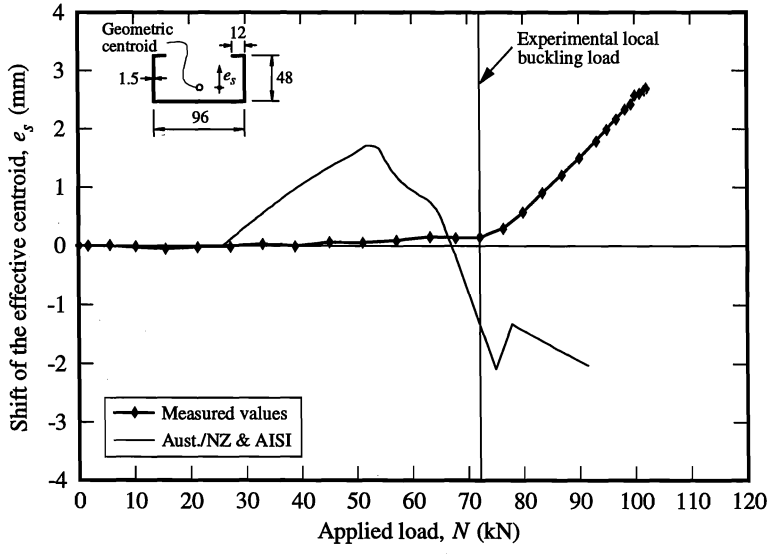

(d) Series L48

Fig. 7. (Cont.) Shift of the effective centroid vs applied load at an effective length of 500mm

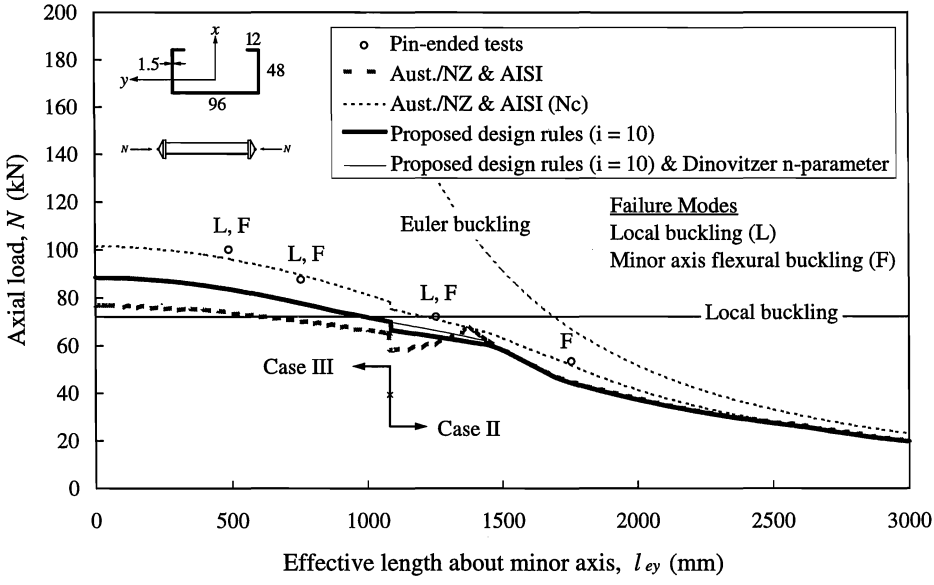

Fig. 8. Comparison of test strengths with current and proposed design strengths for Series L48 section

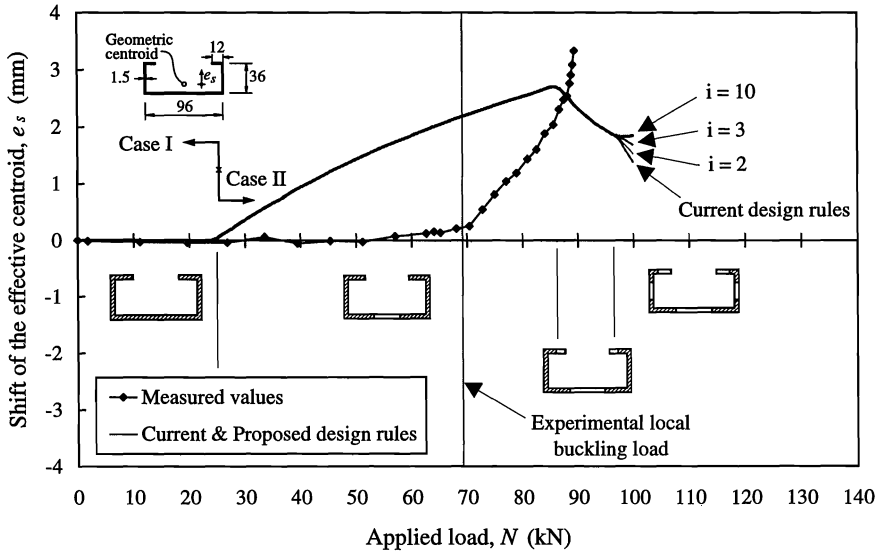

(a) Series L36

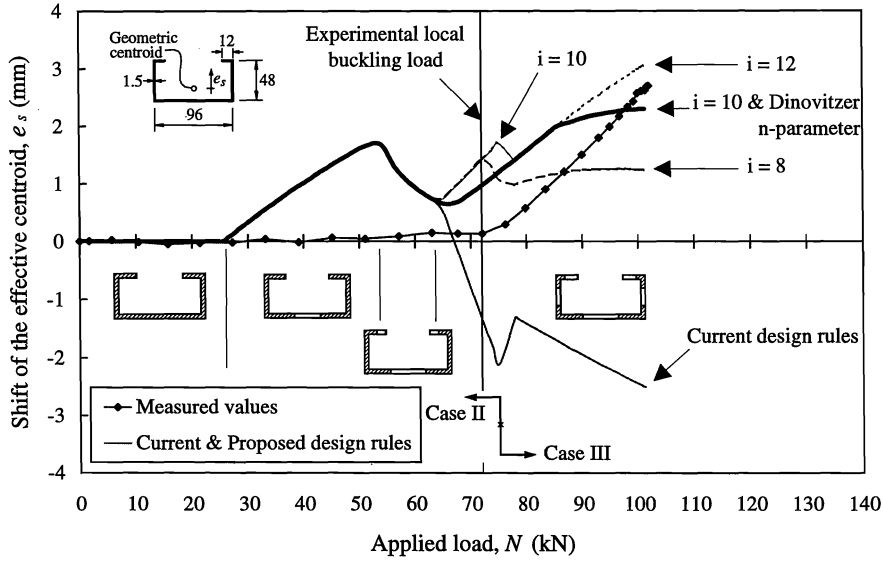

(b) Series L48

Fig. 9. Comparison of measured shift of the effective centroid with current and proposed design rules for lipped channel columns

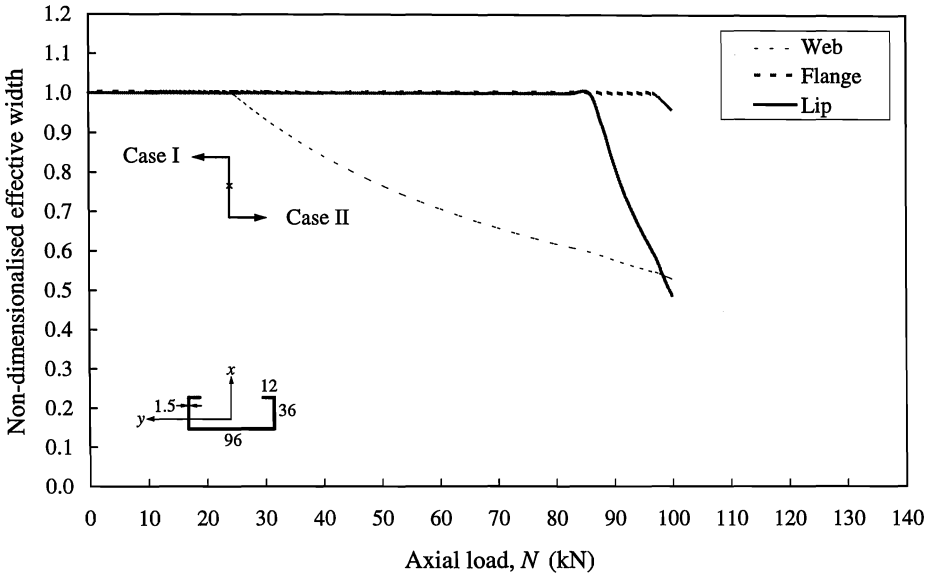

(a) Series L36

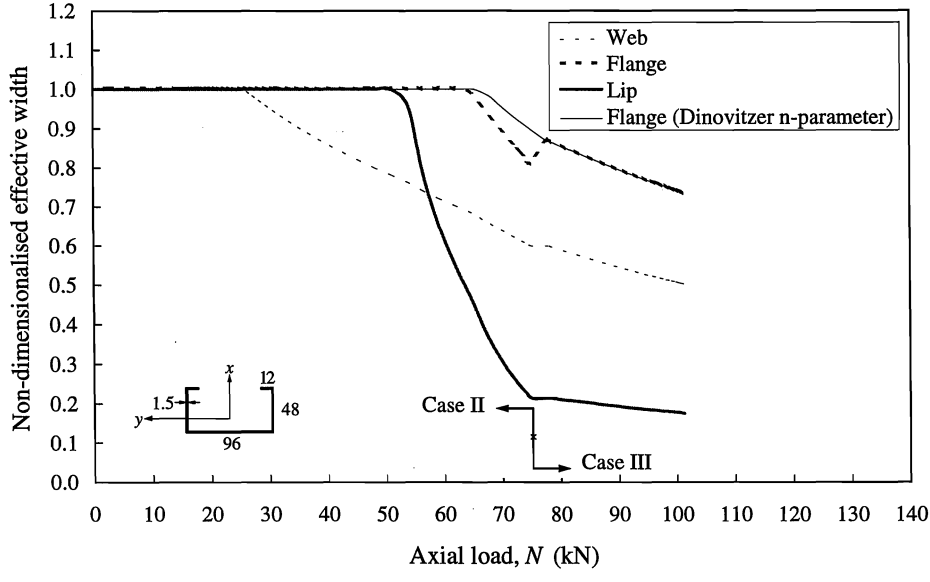

(b) Series L48

Fig. 10. Predicted effective widths of lipped channel columns

Test series	Lips	Flanges	Web	Thickness		Radius	Area
	B_l	B_f	B_w	t	t^*	r_i	A
	(mm)	(mm)	(mm)	(mm)	(mm)	(mm)	(mm^2)
P36	N/A	36.8	96.9	1.51	1.47	0.85	247
P48	N/A	49.6	95.1	1.52	1.47	0.85	282
L36	12.5	37.0	97.3	1.52	1.48	0.85	281
L48	12.3	49.0	97.2	1.51	1.47	0.85	314

Note: 1 in. = 25.4 mm

* Base metal thickness

Table 1. Average measured specimen dimensions

Test series	Nominal	Measured				
	$\sigma_{0.2}$	E	$\sigma_{0.2}$	$\sigma_{0.5}$	σ_u	ε_u
	(MPa)	(GPa)	(MPa)	(MPa)	(MPa)	(%)
P36	450	210	550	560	570	10
P48	450	210	510	525	540	11
L36	450	210	515	525	540	11
L48	450	200	550	560	570	10

Note: 1 ksi = 6.89 MPa

Table 2. Nominal and measured material properties

Effective Length	Exp. Ult. Load	Current Design Strength	Proposed Design Strength ($i = 10$)	Comparison		Improvement
l_{ey}	N_u	$N_{Current}$	$N_{Proposed}$	$\frac{N_u}{N_{Current}}$	$\frac{N_u}{N_{Proposed}}$	$\frac{N_{Proposed}-N_{Current}}{N_{Current}}\times 100$
(mm)	(kN)	(kN)	(kN)			(%)
500	100.1	73.2	83.3	1.37	1.20	13.8
750	87.6	69.9	77.7	1.25	1.13	11.2
1250	72.0	60.2	63.6 [66.2]	1.20	1.13 [1.09]	5.6 [10.0]
1750	53.2	44.3	44.3	1.20	1.20	0

Note: 1 kip = 4.45 kN

[Proposed design rules ($i = 10$) & Dinovitzer n-parameter]

Table 3. Comparison of test strengths with current and proposed design strengths for Series L48